15TH IEA HEAT PUMP CONFERENCE
MAY 26–29, 2026 | HOFBURG
VIENNA 2026
DECARBONISATION THROUGH INNOVATION

Dispatch optimization of high-temperature heat pump technologies for district heating

Nils Hendrik Petersen*, Robert Sager, Manfred Wirsum*

Institute of Power Plant Technology, Steam and Gas Turbines, RWTH Aachen University, Mathieustraße 9, 52074 Aachen, Germany

Abstract

To achieve international climate targets, it is crucial to decarbonise the heating sector. In Germany, heating and cooling account for over 50% of final energy consumption. Significant reductions in greenhouse gas emissions can be realised through electrification via power-to-heat (PtH) technologies. High-temperature heat pumps are a promising PtH solution, potentially providing CO2-free heat supply by utilizing surplus renewable electricity. Numerous studies in the literature analyze the operational planning of heat pumps using mathematical optimization. Often, a generation portfolio is dimensioned for a specific application, such as supplying a district heating network, and the cost-optimal operation of this portfolio is determined while considering electricity market participation.
The novelty of the present study lies in the comparison of different high-temperature heat pump technologies (i.e., transcritical/subcritical) and determination of the techno-economically optimal design of the corresponding heat supply system consisting of the heat pump, an electric boiler, and a heat storage. The analysis includes the technology-dependent coefficient of performance, the ratio of heat provided by heat pump and the electric boiler, and the capacity of the thermal storage system. For the dispatch optimization, a mixed-integer linear programming (MILP) model is formulated. Electricity procurement from the day-ahead and intraday electricity market is considered to meet the representative thermal demand profiles. In addition, technology-dependent partial load operation and dynamic operational characteristics are modeled. The heat supply system designs, the impacts of dynamic operation (i.e., starts, stops, and load changes) as well as electricity procurement are evaluated using the levelized cost of heat (*LCOH*) metric. The results show that part load performance and transient penalties do not have to be considered during dispatch optimization as their impact on the results is comparatively low (<10 %). Moreover, it is shown that *COP* advantages of 10 % can be outperformed by lower *CAPEX.*

Keywords: Model-based analysis; dispatch optimization; levelized cost of heat; flexible operation

1. Introduction

To successfully mitigate climate change, it will be mandatory to decarbonize the heating sector, which accounts for over 50 % of global emissions. In this context, the utilization of Power-to-Heat (PtH) facilities combined with renewable electricity is an essential pillar of a renewable heat supply system. Among PtH technologies, high-temperature heat pumps (HTHP) stand out as a promising option due to their high efficiency and flexibility, especially when coupled with thermal energy storage (TES). Hence, the implementation of HTHP in district heating and industrial applications is already followed [1, 2]. However, the feasibility of a competitive renewable heat supply is constrained by the intermittency and volatility of renewable electricity, as well as by fluctuating electricity prices.

Studies on HTHP can be categorized based on its technical and economic level of complexity (LoC). The technical LoC primarily addresses the analysis and optimization of the Coefficient of Performance (*COP*) and exergetic efficiency under full load design operating conditions (i.e., nominal load at design boundary

* Corresponding author. *E-mail address:* petersen@ikdg.rwth-aachen.de

conditions). Within this scope, numerous studies analyze the effect of cycle design measures such as the implementation of recuperating components (e.g., turbine, internal heat exchanger or ejector) [3, 4] or the serial connection of multiple HTHP. Moreover, the influence of the working fluid and the associated thermodynamic cycle (i.e., sub-, trans-, and supercritical) on the *COP* is widely discussed under varying boundary conditions [5]. Since the legislative framework in the European Union is expected to restrict the use of per- and polyfluoroalkyl substances (PFAS, cf. [6]), current research increasingly focuses on natural refrigerants such as CO_2, ammonia, water and hydrocarbons as working fluids. Nevertheless, hydrofluorolefins (HFOs) continue to be investigated [7]. Research with higher technical LoC expands those analyses for part load (i.e., reduced heat output relative to nominal load) and off-design (i.e., varying boundary conditions) operation as well as the dynamic behavior of the HTHP during load changes [8, 9].

The economic LoC is typically based on variations of the established Net Present Value (*NPV*) method [10]. As illustrated in Eq. (1), the *NPV* represents the difference between the sum of discounted total revenue R_t (i.e., divided by the interest rate to the power of the corresponding year: $(1+i)^t$) over the lifetime T of the HTHP and the initial capital expenditure I_0.

$$NPV = -I_0 + \sum_{t=0}^{T} \frac{R_t}{(1+i)^t} \quad (1)$$

An investment decision is feasible if the sum of discounted cash flows is greater than I_0 (i.e., $NPV > 0$). To determine the cash flow, a market price for heat is required, which is typically not known a-priori (i.e., in theoretical studies without concrete site information). Thus, assuming a *NPV* of zero, Eq. 1 can be reformulated to calculate the Levelized Cost of Heat (*LCOH*), depicting the minimum economically feasible market price for heat [11]. Consequently, *LCOH* is the sum of the discounted capital expenditure (*CAPEX*) and the annual operation expenditure (*OPEX;* i.e., cost flows C_t per heat Q_t) of the HTHP, which is assumed to be constant over the whole lifetime (cf. Eq. 2).

$$LCOH = \frac{I_0 + \sum_{t=1}^{N} \frac{C_t}{(1+i)^t}}{\sum_{t=1}^{N} \frac{Q_t}{(1+i)^t}} = CAPEX + OPEX \quad (2)$$

Alternatively, *NPV* differences can be employed, assuming an identical market price for heat, to compare two investment decisions over a given lifetime [12]. Considering *NPV* differences of zero, the equation can be reformulated to determine a payback period, which indicates a threshold lifetime for one investment to overcome the *NPV* of the other investment [13]. In the case of low economic LoC, all presented variants of the *NPV* are typically evaluated based on seasonal or constant efficiency, loads, boundary conditions and electricity prices. In addition, the impact of seasonal or constant parameters is assessed by conducting sensitivity analyses. To further increase the economic LoC, mathematical optimization methods on deployment and operation strategies are employed in recent studies on HTHP. Within the scope of those studies, a heat supply portfolio is designed for a specific application (e.g., district heating). In a subsequent step, the heat supply portfolio's cost-optimal operation is determined while considering participation in different electricity and balancing power markets (dispatch optimization, cf. [14]).

Currently, research on HTHP tends to lay in a spectrum between an elevated technical LoC without the consideration of economic parameters and dispatch optimization with oversimplified or neglected technological characteristics (e.g., seasonal *COP*, part load operation, and dynamic behavior). However, a previous study by the authors shows that seasonal *COP* and the consideration of part load operation may have considerable impact on the *LCOH* of dispatch optimization in the case of a transcritical CO_2 HP (tCO2-HP) [15]. Nevertheless, a detailed incorporation of part load and transient characteristics has negligible effect on the resulting *LCOH* but increases the computational effort exponentially. Building up on those results, the current study aims to compare the dispatch optimization results of a subcritical Butane HTHP (sC4H10-HP) with the tCO2-HP at the same LoC. The objective is to identify the impact of the working fluid and corresponding thermodynamic cycle of the HTHP on the *LCOH* when operated in combination with an electric boiler and TES.

2. Methods/Approach

A general representation of the HTHP cycles under investigation is displayed in Fig. 1. Subcritical and transcritical Rankine-based HTHP systems are based on the same process steps: The working fluid evaporates (HP4 - HP1) by extracting heat from a heat source (in the present study a sewage water treatment plant) in an evaporator. The evaporated working fluid is then compressed to the upper cycle pressure by a compressor, rising both temperature and pressure (HP1 - HP2). The heat is transferred to a heat sink (in the present study a district heating network) via a gas cooler or a condenser in the case of tCO2 and sC4H10, respectively, (HP2 - HP3). Subsequently, the working fluid is expanded to evaporator pressure (HP3 - HP4). Siemens Energy AG and Everllence SE (former MAN Energy Solutions) are well-established manufacturers for subcritical and tCO2-HP, respectively. In the design of Everllance SE, CO_2 is expanded onto the saturation line via a turbo expander to recuperate mechanical work, followed by an expansion valve for two-phase expansion given the technical challenges of turbomachinery operation in two-phase region. However, for the design of the subcritical process of Siemens Energy AG, no mechanical or thermal recuperation is included. The expansion to the evaporation pressure is facilitated by an expansion valve.

At this point, it shall be mentioned that for both processes, many different cycle configurations exist. However, the focus of the present work is not on cycle design evaluation, but on the combination of high LoC in the technical and economic domain. Thus, the cycle designs displayed in Fig. 1 are deployed for further analyses.

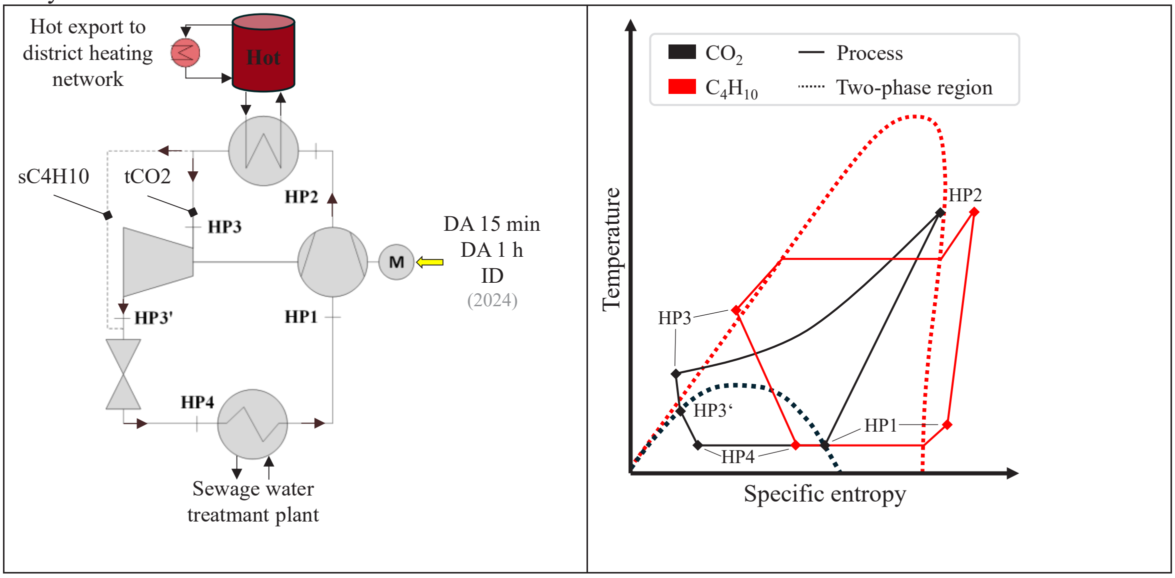

Figure 1: General process flow chart (left) and T-s-diagram (right) of tCO2HP and sC4H10HP

Next to the direct impact on the thermodynamic performance of the HTHP, the choice of working fluid can have significant impact on capital and fixed operational expenditure by its corresponding power densities (i.e., required size of the components) and safety hazards (i.e., flammability and toxicity). A comparison of important properties of CO_2 and Butane is given in Table 1.

Table 1 Fluid properties (selection) of investigated fluids

Medium	Critical pressure [bar]	Critical temperature [K]	Flammability	Toxicity	GWP [-]
CO_2	73.8	304	No	No	1
Butane	38.96	425	High	No	0.006

2.1. Dispatch-optimization

The operation schedule of the HTHP and electric heater (EH) is evaluated for a representative year via dispatch optimization: A Mixed-Integer Linear Programming (MILP) problem is formulated in Python for an optimization of the electricity market-driven operation following technologic boundaries. Therefore, the operation schedule is calculated each day individually and subsequently to maximize total net revenue, which defines the objective function in Eq. (3). R_t equals the total net revenue in time interval t, N equals the total number of intervals, here one year, M equals the total number of markets and i and m are counter variables. p equals the corresponding market prices, while W accounts for the energy charged or discharged on the corresponding market during the corresponding time interval.

For the revenue optimization, the rolling horizon method is applied, assuming a perfect prize forecast of 1.5 days at the beginning of each day. Without the forecast, optimizing a single period would lead to full depletion of the storage at the end of day, which does not necessarily reflect a global optimum. After the optimization process of the period is finished, the optimized schedule for half of the following day is discarded.

$$R_t = \sum_{i=1}^{N}\left(\sum_{m=1}^{M}(p_{dc,m,i} \cdot W_{dc,grid,m,i} - p_{ch,m,i} \cdot W_{ch,grid,m,i})\right) \quad (3)$$

To achieve a feasible solution, the technical and economic framework must be determined: this covers technology specifications of the HTHP and EH (e.g., rated thermal heat and efficiency) as well as the TES (storage size). Moreover, thermodynamic constraints may be specified such as minimal load (thermal turndown), maximum load change rates as well as energy balances. On the economic side, the markets investigated are defined by price-time series. Finally, general information such as solver settings and the investigated time step (in this study: 15 min) are defined. The degrees of freedom of the MILP can be categorized into:

- binary decision variables (e.g., indicating active markets or charging and discharging of the TES) and
- continuous decision variables (e.g., charging or discharging heat flows).

The optimization model is solved using the commercially available Gurobi solver [16]. Further information on the developed model can be found in [17].

The present study considers three energy markets: the Day-Ahead market on a 15-minute and 1-hour basis (DA15/DA1) as well as the continuous Intra-Day market on a 15-minute basis (ID) within the German electricity market framework. Historical price data of the year 2024 is obtained from Entso-E grid operator platform DA1 and DA15 [18] and Energy Charts (ID) [19].

The technical design parameters such as the storage duration, the *COP*, and the electrical power are specified based on available literature data or process calculations.

The part load curve for different heat source temperatures is taken from [9, 20] for the tCO2HP and from [1] for sC4H10HP and displayed in Fig. 2:

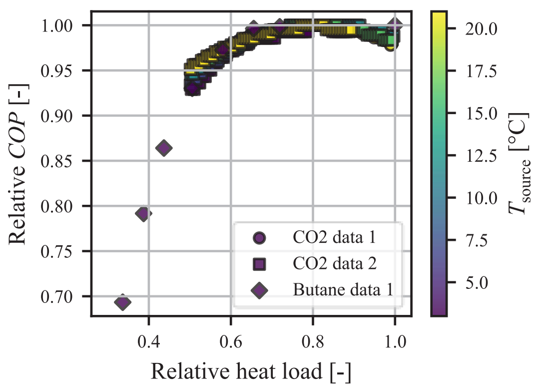

Figure 2 Relative part load curve for efficiency

The y-axis shows the relative *COP* (related to its maximum value at the respective heat source temperature), the x-axis shows the relative thermal capacity. From Fig. 2, it can be seen that between 50 and 100 % load, the relative *COP* is negligibly affected by the current load, varying only between 0.93 and 1. Consequently, the computational efforts in the MILP can be significantly reduced by assuming a constant relative *COP* between 50 and 100 % load. Moreover, for the same supply and return temperature, the relation between the relative variables is negligibly dependent on the heat source temperature and independent of the underlying cycle configuration. Moreover, it can be assumed that the relative *COP* trend is only minorly dependent on return and supply temperature combinations, as it represents the general characteristics of the process: The first CO2 data set is based on 95/40 °C supply and return temperature, while the second CO2 data set is based on 150/45 °C gas cooler inlet and outlet temperature. For the Butane data set, no boundary conditions have been specified. As a result, it is assumed that the relative trends of the *COP* displayed in Fig. 2 can be multiplied with the results from an in-house process calculation tool to obtain boundary condition dependent *COP* as time series.

The process calculation tool deployed in the present study is introduced in [21–23] and is based on a series of energy and mass balances to estimate the state points of the heat pump process. The main technical parameters used are displayed in Table 2.

Table 1: Assumption on technical parameters used in the process calculation tool

Variable	Value	Unit	Reference
Isentropic efficiencies of machinery	0.85	-	assumption
Pinch point temperature difference	5	K	assumption
Cooling of heat source	5	K	assumption
Superheating (sC4H10 process)	15	K	[24, 25]

To estimate transients, publicly available literature on the load change of a tCO2HP is taken from [20]. In their study, Wolscht et al. display experimental and numerical results for transient load changes, from which the following relationship can be withdrawn: a load change between 100 to 30 % rated power takes 30 s. For the sC4H10HP, data is taken from [1]. For a 20,5 MW_{th} heat pump, the cold and hot startup time are 2 and 4 MW_{th}/min, respectively, which corresponds to around 10-20 % load/min. These transient load changes are assumed to be constant over the entire load range and valid for startup and shutdown. As a result, during transients, a linear penalty is applied on the generated heat, depending on the load change rate and the absolute load change. Moreover, from [26], an economic penalty is withdrawn to incorporate the impact of transients on the maintenance cost.

Information on the technical performance of large-scale electrical heaters is taken from [26]. The power of the electrical heater is chosen so that it can always cover the investigated heat load. The heat load profile is assumed to be constant over time and its absolute value is varied between 25, 50 and 75 % of the rated power of the heat pump system, which equals 30 MW_{th}. Thus, the heat load profile can be understood as a capacity factor (*CF*) for the heat supply system.

The storage duration is varied between 2-16 h of charging, which results in a storage capacity between 60-480 MWh_{th}.

The main evaluation parameter in this study is *LCOH* as defined by Eq. (1). The economic lifetime is assumed to be 20 a, the interest rate is equal to 8 %. To account for all other product-related costs such as labor, design, engineering, production, profits and overheads as well as installation and integration cost at the site, the HTHP-related cost is multiplied by the factor 4.16 in accordance with [17]. For the EH, 25 % of the HTHP multiple (i.e., $1.04 \cdot I_{0,\mathrm{HTHP}}$) is assumed for the product-related and integration cost.

From the IEA Annex 58 – Task 1 Technologies [27], the equipment cost can be withdrawn, and a power law relationship can be derived, which is used for further analysis. Thereby, it is assumed that the high specific investment cost i_0 relates to the smaller thermal capacity due to economy of scale reasons. The resulting cost function can be expressed as:

$$i_{0,tCO2} = 1{,}038.4\ \frac{€}{kW_{th}} \cdot \left(\frac{\dot{Q}_{rated}}{1\ kW_{th}}\right)^{-0.317} \tag{4}$$

$$i_{0,sC4H10} = 2{,}439.9\ \frac{€}{kW_{th}} \cdot \left(\frac{\dot{Q}_{rated}}{1\ kW_{th}}\right)^{-0.536} \tag{5}$$

$\dot{Q}_{\mathrm{rated}}$ equals the rated power of the HTHP. The rated power is assumed to equal 30 MW_{th}. The storage costs are estimated based on literature data and on realized projects for pressurized hot water tanks [28–32], assuming a *CAPEX* share of 65 % in accordance with [33]. This leads to the following expression:

$$I_{0,TES} = 1{,}975{,}526\ € + 53{,}418\ € \cdot \left(\frac{V}{1\ m^3}\right)^{0.41} \tag{6}$$

V equals the storage volume and is assessed using the biggest difference between the supply and return temperature and assuming a temperature-independent specific heat capacity equal to 4.18 kJ/kg/K.

The city under investigation in the present study is Flensburg (Germany), as data on the heating network and the outdoor temperature is publicly available. In Fig. 3Figure 3 , time series data for the outdoor temperature, supply temperature and both investigated return temperatures of the district heating network and a sewage water treatment plant temperature are displayed. The y-axis shows the temperature in °C, the x-axis shows the time of the year 2024.

The outdoor temperature can be accessed by the Deutscher Wetterdienst data basis [34]. As there is no weather station in Flensburg, data from Glücksburg is used for Flensburg. This approach is considered valid for the purpose of this study, as the distance between the two cities is less than 10 km. For the district heating network, data on the outdoor, supply and return temperature is available for the years 2014-2016 [35]. From this data, the heating curve is withdrawn, which is subsequently combined with the outdoor temperature of 2024 to derive the supply temperature of 2024. The sewage water treatment plant temperature is taken from publicly available data in Stockholm [26]. No clear trend is observed between the sewage water treatment plant temperature and the outdoor temperature. A comparison of the Stockholm data set with available, yet confidential German data set reveals no qualitative differences. Thus, the Stockholm data set is used for Flensburg under the assumption that the heat source holds enough volume flow to provide the required heat throughout the year.

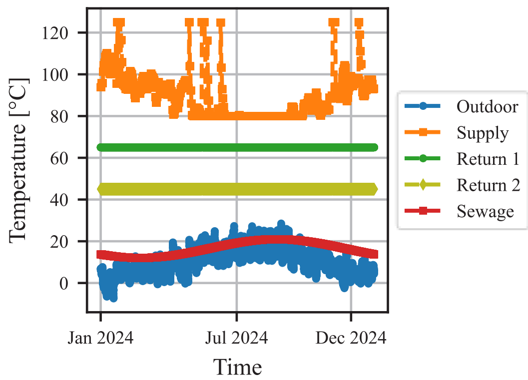

Figure 3 Time series data on outdoor, supply, return and sewage water treatment plant temperature

Using the in-house process calculation tool and the boundary conditions displayed in Fig. 3, the *COP* trend curves are calculated. The results are displayed in Figure 4 .

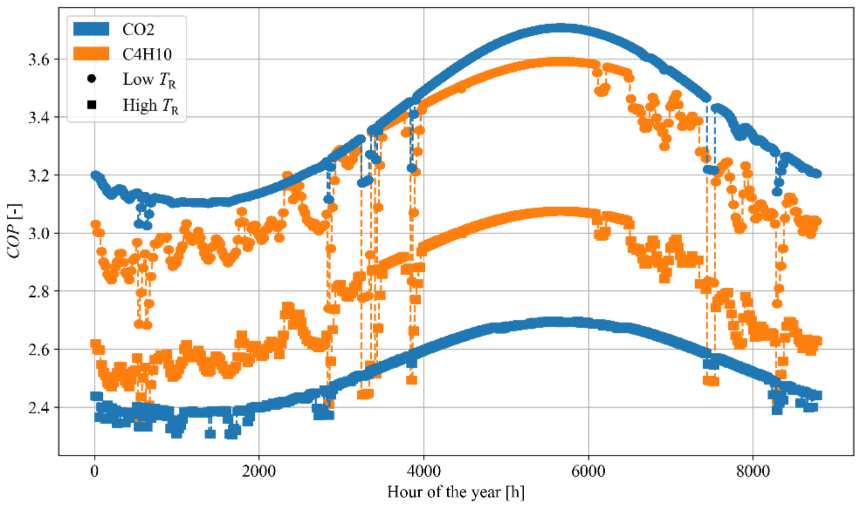

Figure 4 Calculated design *COP* based on temperature boundary conditions

A clearly higher *COP* can be expected for both investigated HTHPs at the low return temperature (LRT), as the mean heat rejection temperature decreases, which in turn leads to higher efficiency following the Lorentz equation [5]. Under the assumptions made in the present study, the *COP* of tCO2HP outperforms sC4H10HP in case of LRT. This can be attributed to the high specific heat capacity of CO_2 close to the critical point, which can be exploited for LRT. In case of the high return temperature (HRT), sC4H10HP outperforms the tCO2HP process as the specific heat capacity of CO_2 cannot be exploited. As a result, the *COP* of tCO2HP decreases significantly. For both return temperatures, it can be observed that tCO2HP is more robust against changes in the supply temperature, as opposed to sC4H10HP: In case of higher supply temperature, subcritical processes must adjust the pressure ratio to provide a sufficiently high condensation temperature, which leads to higher compression efforts and lower condensation enthalpies and thus, to lower *COP*. On the contrary, the tCO2HP process operates optimally at a specific high pressure due to its high mean specific heat capacity, which decouples pressure ratio and supply temperature for a certain supply temperature range and decreases the sensitivity of the *COP*. For further understanding of the following results, the characteristics of the calculated *COP* are displayed in Tab. 3.

Table 32 Calculated COP characteristics

Fluid	T_R	Min.	Max.	Yearly average
CO2	Low	3.03	3.71	3.38
	High	2.30	2.70	2.53
C4H10	Low	2.68	3.59	3.23
	High	2.36	3.08	2.78

3. Results and Discussion

First, a validation of the *COP* estimation method shall be presented. Second, the results for the *LCOH* are evaluated.

3.1. Validation of COP estimation method

To validate the assumption that the seasonal *COP* can be estimated based on design point calculations and subsequently non-dimensionalisation, publicly available data of a tCO2HP from a stationary, part load capable process model is used [9]. The dataset provides information on the season-dependent supply, return and heat source temperature as well as the corresponding *COP*. The results are displayed along with the results obtained using the in-house stationary process calculation tool in Fig. 5.

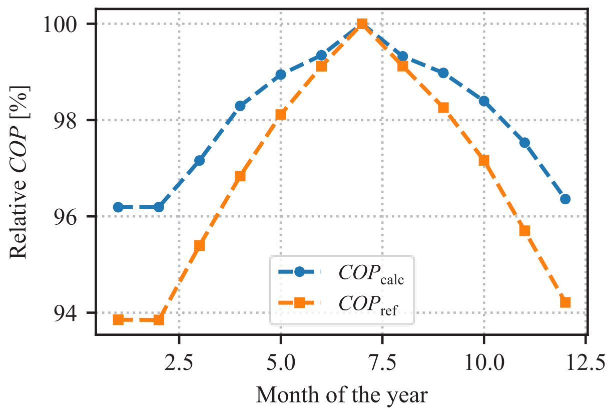

Figure 5: Validation of *COP*-approach

The y-axis shows the relative *COP*, related to the corresponding maximum value of each data set, the x-axis shows the month of the year. The results obtained by the in-house model deviate below 2 %-points throughout the year. This confirms the validity of the chosen *COP*-estimation approach. Nevertheless, it should be mentioned that the absolute *COP* values differ throughout the year with an offset between 0.43 (summer) and 0.49 (winter). The reason lies in non-optimized assumptions regarding component efficiencies, i.e., turbomachinery efficiency and pinch point temperature differences, as well as the heat source outlet temperature. However, the deviation between the in-house tool and the reference is comparatively small because the boundary conditions, i.e., district heating temperatures and heat source temperature, do not change significantly throughout the year. As a result, the turbomachinery can operate close to their design points with only minor impact on overall efficiency. However, if the system operates further away from its design point, e.g., triggered by more notable deviations in the boundary conditions, the chosen modelling approach must be reassessed. Unfortunately, such data set is not available to the authors, so this task is considered as future work. Moreover, no comprehensive dataset on the performance of sC4H10HP is available. Thus, the proposed methodology cannot be validated for sC4H10HP in particular and is considered as future work, too.

3.2. LCOH

The following subsection provides the results obtained by the dispatch optimization tool using the methodology presented above. Fig. 6 and Fig. 7 show the estimated *LCOH* and its absolute composition.

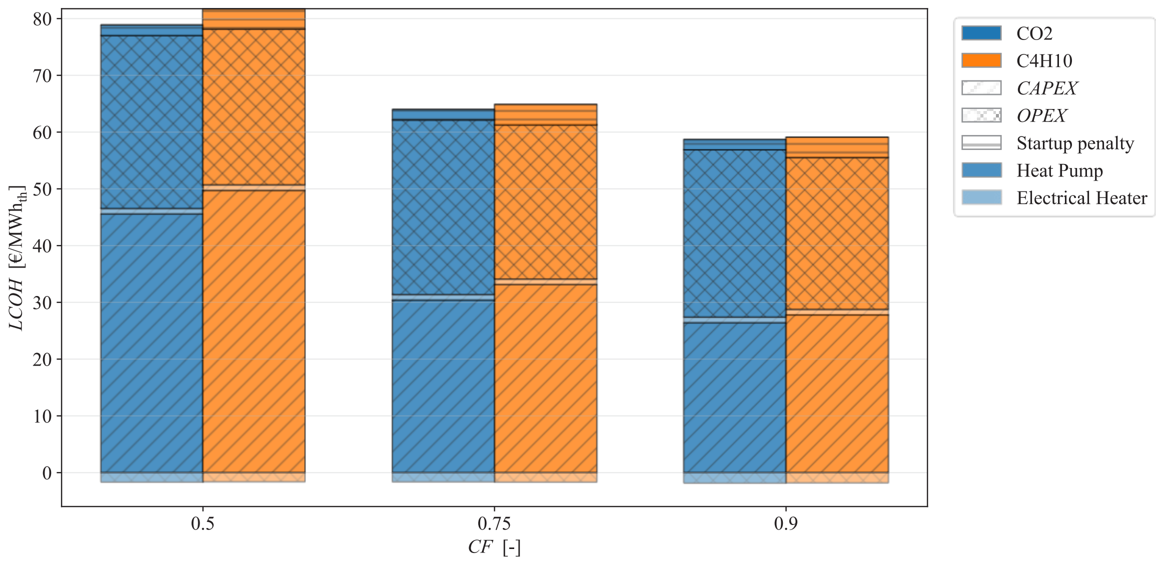

Figure 6 *LCOH* of heat supply system over *CF* for investigated fluids and HRT; *LCOH* composition considering *CAPEX*, *OPEX* and startup penalty is displayed as hatches

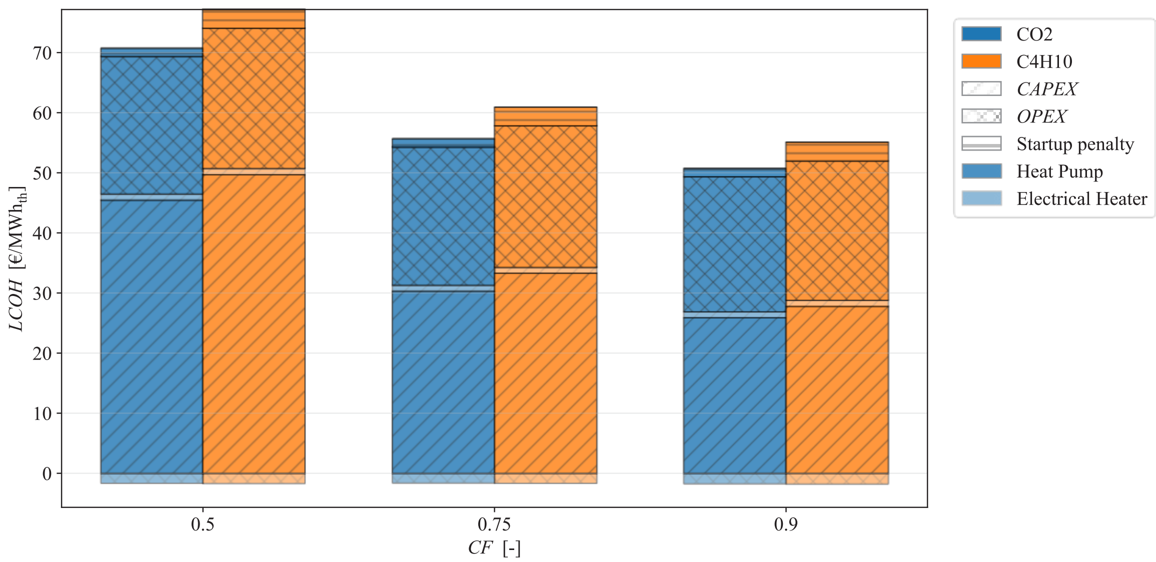

Figure 7 *LCOH* of heat supply system over *CF* for investigated fluids and LRT; *LCOH* composition considering *CAPEX*, *OPEX* and startup penalty is displayed as hatches

The y-axis shows the *LCOH* in €/MWh$_{th}$, the x-axis shows the *CF*. The tCO2HP process is indicated in blue, the sC4H10HP is indicated in orange. The technologies of the heat supply system, i.e., heat pump process and electrical heater, are indicated with full and transparent colors. The composition, i.e., the shares of *CAPEX*, *OPEX* and the startup penalty, are indicated by different hatches.

As expected, *LCOH* decreases with increasing *CF* as the relative share of *CAPEX* of *LCOH* decreases if more heat is generated.

Generally, the impact of the EH on the *LCOH* is comparatively small, ranging from around -0.6 % for *CF*=0.5 to around -0.7 % for *CF*=0.9 for both fluids and both return temperatures. The *LCOH*-reducing impact stems from the relative share of *OPEX* for the electrical heater, which is always negative, it can be derived that the electrical heater is operated preferably at negative electricity prices and for a limited number of hours during low-cost price intervals to further increase storage capacity and avoid high price intervals.

For HRT, tCO2HP outperforms sC4H10HP, with decreasing deviation for increasing *CF*. This finding can be attributed to the *CAPEX*/*OPEX* ratio: As the heat generated for the same *CF* is the same (as the thermal demand profile is constant at $CF \cdot 30\ MW_{th}$), the associated *CAPEX* share of *LCOH* is dependent solely on the *CAPEX* itself. As can be anticipated from Eq. (4) and Eq. (5), sC4H10HP *CAPEX* are higher than for tCO2HP. As a result, the *CAPEX* share of *LCOH* is always higher for sC4H10HP compared to tCO2HP. The *OPEX* share of *LCOH* is lower for sC4H10 in case of HRT and higher in case of LRT. The deviation closely aligns with the yearly averaged *COP*. As a result, *LCOH* of sC4H10HP approaches the tCO2HP for increasing *CF* and HRT, while for LRT, the *LCOH* difference is around 9 %.

Interestingly, the impact of the startup penalty on *LCOH* is almost constant for varying *CF*, but varies according to the assumed numerical value, which is different between both fluids in accordance with [26]. As a result, *CF* ranges between 3.0-3.5 €/MWh_{th} for sC4H10HP and 1.4-1.8 €/MWh_{th} for tCO2HP.
For better reference of the performance of a HTHP+EH system, the individual technology performance in terms of *LCOH* is displayed in Fig. 8

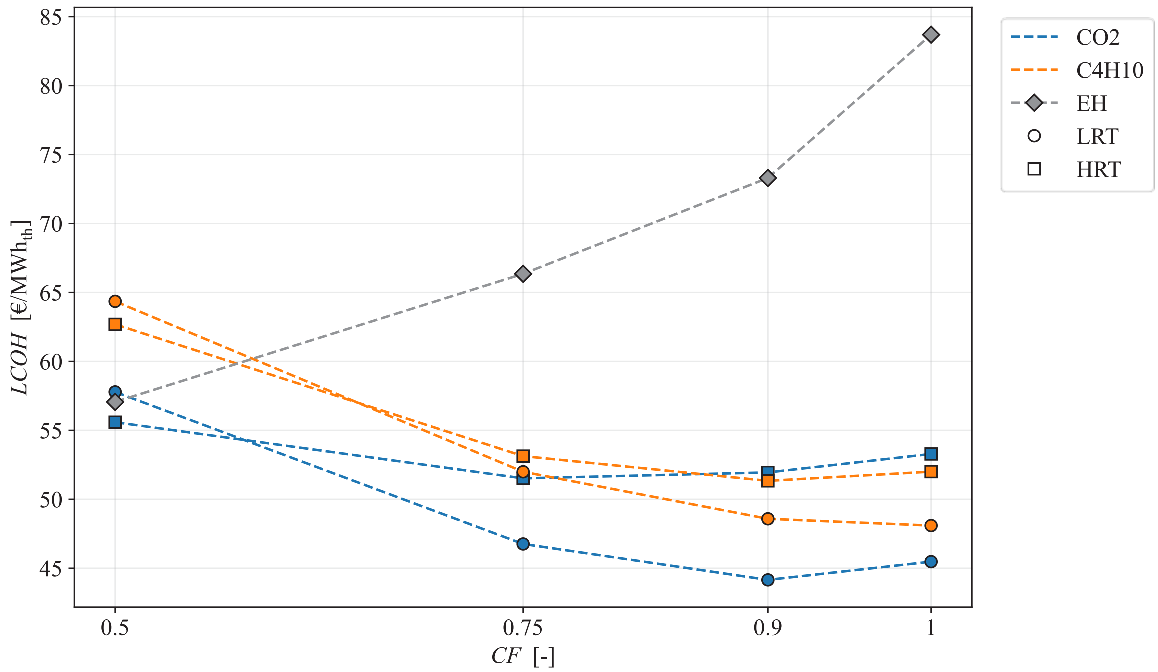

Figure 8 LCOH of individual heat supply system over CF for investigated fluids and both return temperatures

As expected, the electrical heater outperforms all configurations (except CO2-HRT) if *CF* is low enough. For higher *CF*, however, all configurations outperform the EH due to the *COP*-lever. For low *CF*, the inefficient HTHP-HRT-configurations outperform the HTHP-LRT-configurations due to the better use of negative electricity prices, as the former show higher electrical power input for the same thermal power output. Interestingly, the HTHP-configurations always outperform the HTHP-EH-configurations. The reason is that in all cases with $CF < 1$, an oversized HTHP is present. Adding an EH adds *CAPEX*, which is not paid back over continuous operation of the EH as its efficiency is low compared to HTHP. In case of a reduced HTHP size due to the integration of an EH, a *LCOH* benefit could be realized. However, this was not in scope of the present study. Please note that in case of $CF = 1$, no storage cost was assumed.
It is expected that higher storage capacities would lead to higher revenues and lower *LCOH*. However, the results show that each fluid-return temperature-*CF* combination yields an individual optimal storage capacity. The optimal storage capacities obtained are displayed in Table 43.

Table 43 Optimal storage capacity in [h]

Fluid	T_R	CF=0.5	CF=0.75	CF=0.9
CO2	Low	4	4	8
	High	4	4	12
C4H10	Low	8	12	12
	High	8	8	12

Looking at the *LCOH* results, it is found that throughout the storage capacity array investigated (2-16 h), the *LCOH* variation is only within 3.5 % difference. This result might be due to two reasons: first, the storage investment cost is comparatively low (compared to the heat pump expenses), thus an increase in capacity does not necessarily yield higher *LCOH*. Second, the foresight interval in the present study is limited to 0.5 days. It is expected that if foresight is increased, higher storage capacities yield lower *LCOH*, as the additional investment cost is low, but future high-price intervals could be offset with low-price intervals. However, it must be discussed whether perfect foresight within an increased foresight interval is a valid assumption. The investigation of foresight impact on optimal storage capacity is considered as future work.

For future studies, several open questions remain:
- In case of off-design operation, the maximum heat supply can vary, which is not considered in the present study.
- This study shows the impact of the return temperature on the *LCOH*. However, for existing district heating networks, lowering the return temperature correlates with investment at the customers site and heating system, which implicates investment and intensive efforts for the heat supplier.
- In case of fast dynamics, the general startup penalty used might be inaccurate and could have an impact on the economic attractiveness of a startup of the system (i.e., the trade-off between exploiting changes in the electricity procurement cost and economic penalties of transients).
- The current study focuses on the German electricity market framework, which should be expanded to the European level.
- The current study focuses on historical data of 2024, which is assumed constant throughout the lifetime of the heat supply system. This assumption must be challenged, e.g., using electricity price forecasts.
- All other electricity procurement associated costs are neglected in the present study. However, in case of Germany, these costs are considerable [36]
- Different technologies might exhibit different characteristics. It is suggested to expand the view to Joule- and Brayton-based systems as well as different configurations of sub- and transcritical systems.
- The current study has limited data on investment cost and *CAPEX* increasing factors due to construction and commissioning. This gap should be filled in cooperation with experience from OEMs and heat suppliers. In addition, future investment scenarios and possible learning rates should be evaluated regarding the equipment cost.

4. Conclusions

In the present study, two renewable heat supply system consisting of a heat pump technology and an electrical heater with thermal energy storage are compared using a mixed-integer linear programming (MILP) model that considers electricity market participation and technology-dependent operational characteristics.

The technical information is mainly sourced from publicly available data and data from OEMs. Where no data is available, mainly regarding the season-dependent *COP*, an in-house process calculation tool is employed. Its validity is proven using publicly available data.

The results show that both heat supply system show similar economic performance, i.e., *LCOH* between 70-80 €/MWh_{th} for low capacity factor of 50% (*CF*) and 50-60 €/MWh_{th} for high *CF*, depending on the corresponding boundary conditions. The results indicate a slight benefit of the tCO2HP, however, as many assumptions underlie the results, no better performing technology can be clearly identified. It is suggested to further strengthen the assumptions made working together with heating grid operators and operators to further shed light on the techno-economic performance of HTHP.

5. Nomenclature

Variable	Unit	Definition
C_t	€	Cost flow
CF	-	Capacity factor
COP	-	Coefficient of Performance
$CAPEX$	€/MWh_{th}	Capital expenditure
i	%	Interest rate
i_0	€/MW_{th}	Specific investment cost
I_0	€	Investment cost
$LCOH$	€/MWh_{th}	Levelized Cost of Heat
NPV	€	Net present value
p	€/$MWh_{el/th}$	Energy-specific price
$OPEX$	€/MWh_{th}	Operational expenditure
Q	MWh_{th}	Heat
$\dot{Q}$	MW_{th}	Heat flow
R_t	€	Total revenue
T	a	Lifetime
V	m^3	Volume
W	MWh_{el}	Work

6. References

[1] F. Hack and N. Wenn, "Reallabor Großwärmepumpen – Praxisbericht zur Errichtung einer 20 MWth-Flusswärmepumpe in Mannheim," in *Kraftwerkstechnik 2024*, Freiberg: SAXONIA, 2024, pp. 169–180.

[2] Everllence, *Mega Heat Pump Delivers First Heat in Esbjerg.* [Online]. Available: https://www.man-es.com/company/press-releases/press-details/2024/11/28/mega-heat-pump-delivers-first-heat-in-esbjerg (accessed: Nov. 17 2025).

[3] B. Yu, J. Yang, D. Wang, J. Shi, and J. Chen, "An updated review of recent advances on modified technologies in transcritical CO2 refrigeration cycle," *Energy*, vol. 189, p. 116147, 2019, doi: 10.1016/j.energy.2019.116147.

[4] Martin Olafsen, "Optimization and Process Improvements of a High Temperature Heat Pump Using Butane as Working Fluid," Master thesis, NTNU, Trondheim, 2018. [Online]. Available: https://ntnuopen.ntnu.no/ntnu-xmlui/handle/11250/2498758

[5] C. Arpagaus, F. Bless, M. Uhlmann, J. Schiffmann, and S. S. Bertsch, "High temperature heat pumps: Market overview, state of the art, research status, refrigerants, and application potentials," *Energy*, vol. 152, pp. 985–1010, 2018, doi: 10.1016/j.energy.2018.03.166.

[6] European Chemicals Agency (ECHA), *Background Document to the Opinion on the Annex XV dossier proposing restrictions on Per- and polyfluoroalkyl substances (PFASs).* [Online]. Available: https://echa.europa.eu/documents/10162/17233/rest_pfas_bd_draft_240625_en.pdf/86488ab5-30c9-f7b9-547d-84db15535d9a?t=1755590462498 (accessed: Nov. 17 2025).

[7] C. Mateu-Royo, C. Arpagaus, A. Mota-Babiloni, J. Navarro-Esbrí, and S. S. Bertsch, "Advanced high temperature heat pump configurations using low GWP refrigerants for industrial waste heat recovery: A comprehensive study," *Energy Conversion and Management*, vol. 229, p. 113752, 2021, doi: 10.1016/j.enconman.2020.113752.

[8] L. Wolscht, M. Podeur, M. Adams, and E. Jacquemoud, "Off-Design Heat Exchanger Modelling for Transcritical CO2 Heat Pump Cycles," in *Proceedings of ASME Turbo Expo 2024: Turbomachinery Technical Conference and Exposition (GT2024): June 24-28, 2024, London, United Kingdom*, London, United Kingdom, 2024.

[9] P. Gabrielli, G. Sansavini, S. Singh, L. S. Garcia, E. Jacquemoud, and P. Jenny, "Off-Design Modeling and Operational Optimization of Trans-Critical Carbon Dioxide Heat Pumps," *Journal of Engineering for Gas Turbines and Power*, vol. 144, no. 10, 2022, doi: 10.1115/1.4055233.

[10] A. Kijo-Kleczkowska, P. Bruś, and G. Więciorkowski, "Economic analysis of heat pump exploitation – A case study," *Energy*, vol. 280, p. 128184, 2023, doi: 10.1016/j.energy.2023.128184.

[11] E. Vieren, K. Couvreur, M. de Paepe, and S. Lecompte, "High-temperature heat pumps in industrial heating networks: A study on energy use, emissions, and economics," *Applied Thermal Engineering*, vol. 259, p. 124799,

2025, doi: 10.1016/j.applthermaleng.2024.124799.
[12] A. Vannoni, A. Sorce, A. Traverso, and A. Fausto Massardo, "Techno-economic optimization of high-temperature heat pumps for waste heat recovery," *Energy Conversion and Management*, vol. 290, p. 117194, 2023, doi: 10.1016/j.enconman.2023.117194.
[13] H. Sadeghi, A. Ijaz, and R. M. Singh, "Current status of heat pumps in Norway and analysis of their performance and payback time," *Sustainable Energy Technologies and Assessments*, vol. 54, p. 102829, 2022, doi: 10.1016/j.seta.2022.102829.
[14] S. Siddiqui, J. Macadam, and M. Barrett, "The operation of district heating with heat pumps and thermal energy storage in a zero-emission scenario," *Energy Reports*, vol. 7, pp. 176–183, 2021, doi: 10.1016/j.egyr.2021.08.157.
[15] N. H. Petersen, R. Sager, and M. Wirsum, "The impact of level of complexity in techno-economic analysis of high temperature heat pumps," in *3. Konferenz der Norddeutschen Wärmeforschung*.
[16] L. L. Gurobi Optimization, *Gurobi Optimizer Reference Manual.* [Online]. Available: https://www.gurobi.com/
[17] N. H. Petersen, M. Wirsum, D. Kodz, and K. Iranshahi, "Trigeneration driven design of a transcritical CO2 Carnot Battery," in *Proceedings of ECOS2025*.
[18] European TSOs, *Day-ahead Prices*.
[19] Fraunhofer ISE, *Stromproduktion und Börsenstrompreise in Deutschland 2023*.
[20] L. Wolscht, R. Somaini, E. Jacquemoud, and P. Jenny, "Full-Scale Demonstration and Validation of a 35 MW Transcritical CO2 Heat Pump," in *Proceedings of ASME Turbo Expo 2023: Turbomachinery Technical Conference and Exposition (GT 2023): June 26-30, 2023, Boston, Massachusetts*, Boston, Massachusetts, USA, 2023.
[21] N. H. Petersen *et al.,* "Nutzung transkritischer CO2-Prozesse für Wärmepumpen und elektro-thermische Energiespeicher," in *Kraftwerkstechnik 2021*, M. Beckmann and A. Hurtado, Eds., Freiberg: SAXONIA, 2021, pp. 1388–1403.
[22] N. H. Petersen *et al.,* "Potentialanalyse der Nutzung transkritischer Co2-Prozesse zur Fern- und Industriewärmebereitstellung in Nordrhein-Westfalen," in *17. Symposium Energieinnovation 2022*, pp. 1–13. [Online]. Available: https://www.tugraz.at/fileadmin/user_upload/tugrazExternal/738639ca-39a0-4129-b0f0-38b384c12b57/files/lf/Session_E4/542_Petersen_v2.pdf
[23] N. H. Petersen, M. Arras, M. Wirsum, and L. Ma, "Integration of large-scale heat pumps to assist sustainable water desalination and district cooling," *Energy*, vol. 289, p. 129733, 2024, doi: 10.1016/j.energy.2023.129733.
[24] VERDNIK M., RIEBERER R., and MOISI H., "Trans-critical vapor compression cycle using butane (R600) as refrigerant for industrial waste heat recovery," 2019.
[25] M. Verdnik and R. Rieberer, "Influence of operating parameters on the COP of an R600 high-temperature heat pump," *International Journal of Refrigeration*, vol. 140, pp. 103–111, 2022, doi: 10.1016/j.ijrefrig.2022.05.010.
[26] Danish Energy Agency, *Technology Data - Energy Plants for Electricity and District heating generation*, 2016.
[27] Benjamin Zühlsdorf *et al., IEA HPT Annex 58: High-Temperature Heat Pumps. Task 1 report: Technologies*, 2023.
[28] H. Weckbrodt, "Drewag Dresden startet neuen Wärmeenergie-Speicher," *Oiger*, 30 Nov., 2018. https://oiger.de/2018/11/30/drewag-dresden-startet-neuen-waermeenergie-speicher/170067 (accessed: Oct. 14 2025).
[29] S. Mati, "Wärmespeicher sichert günstige Preise für Fernwärme - Unser Hürth," 03 Oct., 2019. https://www.unserhuerth.de/2019/08/21/waermespeicher-sichert-guenstige-preise-fuer-fernwaerme/ (accessed: Oct. 14 2025).
[30] A. Kraft and M. Maximini, "Wärmespeicher für Nah- und Fernwärmenetze," 2021.
[31] A. C. Christidis *et al., EnEff:Wärme - Einsatz von Wärmespeichern und Power-to-Heat-Anlagen in der Fernwärmeerzeugung* (in ger), Forschung und Entwicklung / AGFW. Frankfurt am Main: AGFW, vol. 44.
[32] M. Morandin, M. Mercangöz, J. Hemrle, F. Maréchal, and D. Favrat, "Thermoeconomic design optimization of a thermo-electric energy storage system based on transcritical CO2 cycles," *Energy*, vol. 58, pp. 571–587, 2013, doi: 10.1016/j.energy.2013.05.038.
[33] European Commission. Joint Research Centre., ILF Consulting Engineers Austria GmbH., and AIT Austrian Institute of Technology GmbH., *Long term (2050) projections of techno-economic performance of large-scale heating and cooling in the EU*: Publications Office, 2017.
[34] *Index of /climate_environment/CDC.* [Online]. Available: https://opendata.dwd.de/climate_environment/CDC/ (accessed: Oct. 14 2025).
[35] Stadtwerke Flensburg GmbH, *District heating network data for the city of Flensburg from 2014-2016*: Zenodo. [Online]. Available: https://zenodo.org/records/2562658
[36] Agora Energiewende and Fraunhofer IEG, "Roll-out von Großwärmepumpen in Deutschland: Strategien für den Markthochlauf in Wärmenetzen und Industrie," 2023.